

Coordination Properties of Ionic Liquid-Mediated Chromium(II) and Copper(II) Chlorides and Their Complexes with Glucose

Evgeny A. Pidko,* Volkan Degirmenci, Rutger A. van Santen, and Emiel J. M. Hensen*

Schuit Institute of Catalysis, Eindhoven University of Technology, P.O. Box 513, NL-5600 MB, Eindhoven, The Netherlands

Received July 14, 2010

The structural and coordination properties of complexes formed upon the interaction of copper(II) and chromium(II) chlorides with dialkylimidazolium chloride (RMI⁺Cl⁻) ionic liquids and glucose are studied by a combination of density functional theory (DFT) calculations and X-ray absorption spectroscopy (XAS). In the absence of the carbohydrate substrate, isolated mononuclear four-coordinated MeCl₄²⁻ species (Me = Cu, Cr) dominate in the ionic liquid solution. The organic part of the ionic liquid does not directly interact with the metal centers. The interactions between the RMI⁺ cations and the anionic metal chloride complexes are limited to hydrogen bonding with the basic Cl⁻ ligands and the overall electrostatic stabilization of the anionic metal complexes. Exchange of Cl⁻ ligands by a hydroxyl group of glucose is only favorable for CrCl₄²⁻. For Cu²⁺ complexes, the formation of hydrogen bonded complexes between CuCl₄²⁻ and glucose is preferred. No preference for the coordination of metal chloride species to specific hydroxyl group of the carbohydrate is found. The formation of binuclear metal chloride complexes is also considered. The reactivity and selectivity patterns of the Lewis acid catalyzed reactions of glucose are discussed in the framework of the obtained results.

1. Introduction

Concerns about global warming, energy security, and declining oil resources are the main drive for the extensive studies both in industry and academia aimed at developing alternative and more sustainable routes for the production of chemicals and fuels. Lignocellulosic biomass is recognized a promising renewable and carbon-neutral source of platform substances for the productions of fuels and bulk chemicals.¹ The efficient utilization of biomass requires development of new catalytic routes for selective transformation of carbohydrates into desirable chemicals with a wide range of downstream applications.^{2,3} 5-Hydroxymethylfurfural (HMF) is regarded as a versatile platform molecule.⁴

Although HMF can be produced from fructose by using a wide variety of catalysts,^{5–9} its selective formation from glucose is challenging. Only recently, an unprecedented HMF yield of 70% was reported for the dehydration of glucose by CrCl₂ in 1-ethyl-3-methylimidazolium chloride (EMIm⁺Cl⁻) ionic liquid.⁹ In general, the vast majority of studies reporting successful catalytic transformations of glucose to HMF deal with the ionic liquid-mediated chromium catalysis.^{9–12} In addition, SnCl₄ in 1-ethyl-3-methylimidazolium tetrafluoroborate (EMIm⁺BF₄⁻) was also shown to be promising for glucose dehydration.¹³ However, the HMF selectivities reported were substantially lower in this case compared to those obtained by CrCl₂. Other Lewis acid catalysts, such as for example CuCl₂, can promote glucose conversion, but give mainly condensation products and show very low selectivities to HMF.⁹

In our recent communication,¹⁴ we investigated the mechanism of glucose dehydration in CrCl₂/EMIm⁺Cl⁻ system by a combination of kinetic experiments, in situ X-ray absorption spectroscopy (XAS) and DFT calculations. It was demonstrated that the unique catalytic performance of

*To whom correspondence should be addressed. E-mail: e.a.pidko@tue.nl (E.A.P.); e.j.m.hensen@tue.nl (E.J.M.H.). Tel: +31 40 247 2189 (E.A.P.); +31 40 247 5178 (E.J.M.H.).

(1) Centi, G. C.; van Santen, R. A., Eds. *Catalysis for Renewables: From Feedstock to Energy Production*; Wiley-VCH: Weinheim, Germany, 2007.

(2) Huber, G. W.; Iborra, S.; Corma, A. *Chem. Rev.* **2006**, *106*, 4044.

(3) Corma, A.; Iborra, S.; Velty, A. *Chem. Rev.* **2007**, *107*, 2411.

(4) Chheda, J. N.; Huber, G. W.; Dumesic, J. A. *Angew. Chem., Int. Ed.* **2007**, *46*, 7164.

(5) Asghari, F. S.; Yoshida, H. *Carbohydr. Res.* **2006**, *341*, 2379.

(6) Qi, X. H.; Watanabe, M.; Aida, T. M.; Smith, R. L. *ChemSusChem* **2009**, *2*, 944.

(7) Sievers, C.; Musin, I.; Marzalletti, T.; Olarte, M. B. V.; Agrawal, P. K.; Jones, C. W. *ChemSusChem* **2009**, *2*, 665.

(8) Chheda, J. N.; Roman-Leshkov, Y.; Dumesic, J. A. *Green Chem.* **2009**, *9*, 342.

(9) Zhao, H.; Holladay, J. E.; Brown, H.; Zhang, Z. C. *Science* **2007**, *316*, 1597.

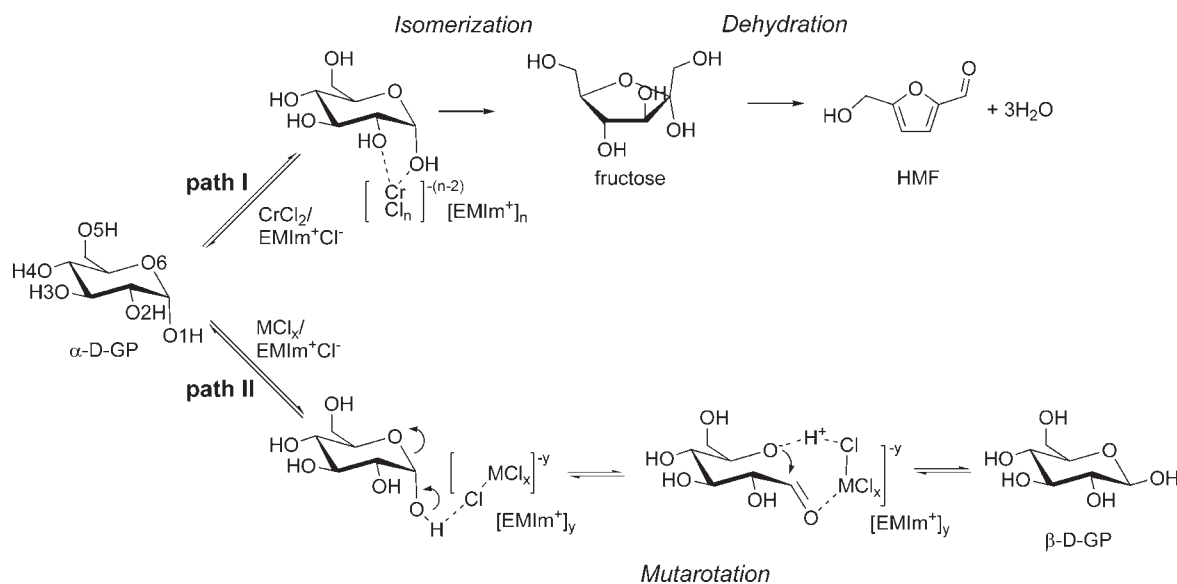
(10) Yong, G.; Zhang, Y. G.; Ying, J. Y. *Angew. Chem., Int. Ed.* **2008**, *47*, 9345.

(11) Binder, J. B.; Raines, R. T. *J. Am. Chem. Soc.* **2009**, *131*, 1979.

(12) Li, C.; Zhang, Z.; Zhao, Z. K. *Tetrahedron Lett.* **2009**, *50*, 5403.

(13) Hu, S.; Zhang, Z.; Song, J.; Zhou, Y.; Han, B. *Green Chem.* **2009**, *11*, 1746.

(14) Pidko, E. A.; Degirmenci, V.; van Santen, R. A.; Hensen, E. J. M. *Angew. Chem., Int. Ed.* **2010**, *49*, 2530.

Scheme 1. Tentative Scheme for the Reactive Interactions of Glucose with Metal Halides in EMIm⁺Cl⁻ Ionic Liquid Proposed by Zhang et al.^{9 a}

^aThe suggested direct interaction between the anionic metal chloride complex and EMIm⁺ cation⁹ in the reactive complex is omitted in view of the results presented above.

CrCl₂ in EMIm⁺Cl⁻ is the result of the ability of this catalyst to promote isomerization of glucose to fructose. The transient self-organization of Cr²⁺ complexes into dimers in the course of the catalytic reaction promotes the glucose to fructose isomerization step that determines the overall HMF selectivity. The specific reaction environment providing sufficient mobility of the Cr complexes and the basic Cl⁻ sites is crucial to obtain high yields of HMF.^{14,15} The structure of the active complex at the rate limiting step resembles the active site of hexose isomerase enzymes.^{16,17}

Glucose activation by CrCl₂/EMIm⁺Cl⁻ requires coordination of the sugar molecule to the chromium center via O1H and O2H hydroxyl groups (Scheme 1). Such a coordination mode allows efficient stabilization of various anionic reaction intermediates formed in the course of the isomerization reaction.¹⁴ In enzymatic systems, on the contrary, another binding mode, namely, via O3H and O4H hydroxyls, to the metal cofactors is considered to be relevant.¹⁶ In this case, the Lewis acidic sites do not directly promote the initial activation of the carbohydrate substrate.

Zhang et al.⁹ suggested a tentative scheme for reactive interactions of glucose with metal halides in EMIm⁺Cl⁻ leading to its isomerization and dehydration. Two distinct interaction modes were proposed (Scheme 1) to be responsible for the mutarotation (path I) and isomerization/dehydration reaction paths (path II). For both pathways, a MeCl₃⁻EMIm⁺ species was proposed as the active metal complex involving also a direct interaction of the metal center (Me) with the cationic part of the ionic liquid (EMIm⁺). For glucose mutarotation, no direct coordination between the OH groups of the sugar and the Lewis acidic species is required at the initial step of the reaction (path I,

Scheme 1). According to the scheme proposed,⁹ basic Cl⁻ ligands of the MeCl₃⁻EMIm⁺ species directly catalyze proton transfer between the O1 and O6 sites of glucose, resulting in the opening of the glucopyranose ring and mutarotation. For the isomerization and dehydration pathway (path II, Scheme 1), a crucial role of the specific bidentate O1,O2-coordination mode to the Cr²⁺ center was suggested. A similar mechanism has been proposed to explain the catalytic activity of the SnCl₄/EMIm⁺BF₄⁻ catalyst.¹³ However, no direct evidence for the preference of such a particular coordination mode is available.

Molecular level insight into the structural and coordination properties of metal chlorides and their complexes with glucose in the ionic liquid medium is necessary for further improvement of these catalytic systems. To the best of our knowledge, so far properties of only a limited number of pure metal chlorides in ionic liquids have been investigated in significant details, whereas detailed molecular-level information on sugar interactions in such systems is not available. AlCl₃-containing ionic liquids are among the most widely studied systems. The catalytic properties of these ionic liquids are mainly determined by the chloroaluminate anionic species. Their structural properties have been widely characterized by NMR spectroscopy,^{18–22} Raman, UV and IR spectroscopies as well as electrochemical methods.^{21–25} The presence of the mono- and binuclear anions, respectively AlCl₄⁻ and Al₂Cl₇⁻, has been shown. Imidazolium salts of other

(15) Degirmenci, V.; Pidko, E. A.; Hensen, E. J. M. Submitted for publication.

(16) Fenn, T. D.; Ringe, D.; Petsko, G. A. *Biochem.* **2004**, *43*, 6464.

(17) Meilleur, F.; Snell, E. H.; van der Woerd, M. J.; Judge, R. A.; Myles, D. A. A. *Eur. Biophys. J.* **2006**, *35*, 601.

(18) Yoo, K.; Namboodiri, V. V.; Varma, R. S.; Smirniotis, P. G. *J. Catal.* **2004**, *222*, 511.

(19) Gu, Y.; Shi, F.; Deng, Y. *J. Mol. Catal. A: Chem.* **2004**, *212*, 71.

(20) Woodcock, C.; Shriver, D. F. *Inorg. Chem.* **1986**, *25*, 2137.

(21) Zawadzinski, J. T. A.; Osteryoung, R. A. *Inorg. Chem.* **1989**, *28*, 1710.

(22) Chauvin, Y.; Di Marco-Van Tiggelen, F.; Olivier, H. *J. Chem. Soc., Dalton Trans.* **1993**, 1009.

(23) Angell, C. A.; Bennett, P. D. *J. Am. Chem. Soc.* **1982**, *104*, 6304.

(24) Gilbert, B.; Chauvin, Y.; Guibard, I. *Vib. Spectrosc.* **1991**, *1*, 299.

(25) Chauvin, Y.; Olivier, B. H.; Wyrvalski, C.; Simon, L. C.; de Souza, R. F. *J. Catal.* **1997**, *165*, 275.

metal chlorides such as iron,^{26–28} tin,^{27,29} zinc,^{27,29–31} copper,²⁷ nickel,³² cobalt,³² manganese,²⁷ hafnium, and zirconium³³ in dialkylimidazolium-based ionic liquids have also been studied. Most of the structural information on the metal chloride complexes was obtained by single crystal X-ray diffraction (XRD). XRD data on cocrystals of CuCl₂²⁷ and CrCl₂³⁴ with RMIm⁺Cl[−] ionic liquids have also been reported. It was demonstrated that whereas in the case of copper(II) isolated perturbed tetrahedral CuCl₄^{2−} complexes are formed,²⁷ chromium(II) tends to form chain structures build from distorted octahedral Cr²⁺ chloride complexes.³⁴ In both cases, the RMIm⁺ cations provide an efficient charge-compensating environment for the anionic metal chloride complexes. No coordination of the RMIm⁺ to metal centers was observed.

It is difficult to obtain direct information on the state, nuclearity, and coordination properties of ionic liquid-mediated metal chloride complexes. Herein, we report a combined density functional theory (DFT) and in situ X-ray absorption spectroscopy (XAS) study aimed at the detailed comparative analysis of structural and coordination properties of copper(II) and chromium(II) chlorides and their complexes with glucose in RMIm⁺Cl[−] ionic liquids.

2. Computational and Experimental Details

2.1. DFT Calculations. Density functional theory (DFT) with the PBE0 (also denoted as PBE1PBE and PBEh)³⁵ hybrid exchange-correlation functional was used for the quantum chemical calculations. Prior benchmark studies have shown the high accuracy of this method among a set of hybrid exchange-correlation functionals for the description of a wide

range of systems³⁶ such as transition metal catalyzed reactions³⁷ and magnetic systems.³⁸ Full geometry optimizations and saddle-point searches were performed within Gaussian 03.³⁹ For geometry optimization and frequency analysis the full electron 6-31+G(d) basis set was used for Cr, Cl, and O atoms. The C, N, and H atoms were treated with the 6-31G(d) basis set. Such a basis set combination allowed accurate calculation of extended molecular models considered in this study. To justify the use of such a basis set combination, test calculations involving geometry optimization of selected models discussed in this work were performed using an extended combination of basis sets, in which Cr atoms were treated using the 6-311+G(3df) basis set, the Cl, C, H, and O atoms of the carbohydrate molecule and its derivatives were described with the 6-311++G(d,p) basis set, and the 6-311G(d,p) basis set for the remaining C, H, and N atoms of the 1,3-dimethylimidazolium (MMIm) cation of the model ionic liquid solvent. The deviation in relative energies of isomeric glucose···CrCl₃[−] complexes compared to the values obtained using the standard procedure did not exceed 3 kJ mol^{−1}. The effect of the extended combination of basis sets on the geometrical properties of the optimized structures was negligible. The Cr²⁺ and Cu²⁺ complexes were in high spin-state ($S = 4/2$ and $S = 8/2$ for mononuclear and binuclear Cr complexes, respectively, and $S = 1/2$ and $S = 3/2$ for mononuclear and binuclear Cu complexes, respectively). The choice of the spin state is supported by previous studies on Cr(II) chlorides⁴⁰ and the results of magnetic susceptibility measurements (see Supporting Information). Atomic charges were computed with the Natural Bond Orbital (NBO) method as implemented in the Gaussian 03 program package. The total charge of all molecular models was 0. The initial configurations of charge-compensating dialkylimidazolium cations were constructed based on the structure of the CrCl₂·EMIm⁺Cl[−] cocrystal determined by single-crystal XRD.³⁴

The nature of the stationary points was evaluated from the harmonic modes analytically computed using a complete Hessian matrix for all models. No imaginary frequencies were found for the optimized structures, confirming that these correspond to local minima on the potential energy surface.

Zero point (E_{ZPE}), finite temperature (H_{CORR}), and entropic (TS) energy contributions were computed using the results of the normal-mode analysis within the ideal gas approximation at a pressure of 1 atm and temperatures of 298, 353, and 373 K. To reduce potential errors associated with the nonuniform stabilization and charge-compensation of the MMIm⁺ ions at the outer part of the molecular models, only the contribution of the MeCl_n species and the carbohydrate molecule and its derivatives were considered in calculations of the thermodynamic properties. The contributions of the atoms of the charge-compensating MMIm⁺ ions were removed from the Hessian matrix for all structures in this case. The values of ΔG° were calculated for these conditions.

2.2. Materials. Commercially available D-glucose (Sigma-Aldrich, >99.5%), 1-ethyl-3-methylimidazolium chloride (Merck, >98%), Cr^{II}Cl₂ (Sigma-Aldrich, 99.99%) and Cu^{II}Cl₂ (Merck, >98%) were used in this study. Because of the extreme sensitivity of the Cr²⁺ compounds to air, all manipulations and preparations were performed with great care in a nitrogen-flushed glovebox with oxygen concentration not exceeding 1 ppm. All necessary precautions to avoid contact with oxygen during the spectroscopic measurements were taken.

2.3. XAS Experiments. X-ray absorption spectroscopy (XAS) experiments were performed in a small home-built cell that contains the liquid and that can be heated up to 200 °C. The liquid was placed between Kapton windows. XAS spectra were collected in fluorescence mode at the Cr and Cu K edges at the

(26) Sitze, M. S.; Schreiter, E. R.; Patterson, E. V.; Freeman, R. G. *Inorg. Chem.* **2001**, *40*, 2298.

(27) Zhong, C.; Sasaki, T.; Jimbo-Kobayashi, A.; Fujiwara, E.; Kobayashi, A.; Tada, M.; Iwasawa, Y. *Bull. Chem. Soc. Jpn.* **2007**, *80*, 2365.

(28) Chen, X.; Peng, Y. *Catal. Lett.* **2008**, *122*, 310.

(29) Abbott, A. P. *ChemPhysChem* **2004**, *5*, 1242.

(30) Ballivet-Tkatchenko, D.; Picquet, M.; Solinas, M.; Francio, G.; Wasserscheid, P.; Leitner, W. *Green Chem.* **2003**, *5*, 232.

(31) Lecocq, V.; Graille, A.; Santini, C. C.; Baudouin, A.; Chauvin, Y.; Basset, J.-M.; Bouchu, D.; Fenet, B. *New J. Chem.* **2005**, *29*, 700.

(32) Hitchcock, P. B.; Seddon, K. R.; Welton, T. *J. Chem. Soc., Dalton Trans.* **1993**, 2639.

(33) Campbell, P. S.; Santini, C. C.; Bouchu, B.; Fenet, B.; Rycerz, L.; Chauvin, Y.; Gaune-Escard, M.; Bessada, C.; Rollet, A.-L. *J. Chem. Soc., Dalton Trans.* **2010**, *39*, 1379.

(34) Danford, J. J.; Arif, A. M.; Berreau, L. M. *Acta Cryst. E* **2009**, *65*, M227.

(35) Adamo, C.; Barone, V. *J. Chem. Phys.* **1999**, *110*, 6158.

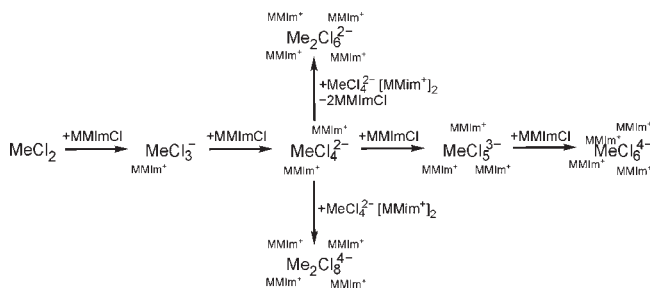
(36) Zhao, Y.; Truhlar, D. G. *Acc. Chem. Res.* **2008**, *41*, 157.

(37) Zhao, Y.; Truhlar, D. G. *J. Chem. Theory Comput.* **2009**, *5*, 324.

(38) Valero, R.; Costa, R.; Moreira, I. de P.R.; Truhlar, D. G.; Illas, F. *J. Chem. Phys.* **2008**, *128*, 114103.

(39) Frisch, M. J.; Trucks, G. W.; Schlegel, H. B.; Scuseria, G. E.; Robb, M. A.; Cheeseman, J. R.; Montgomery, J. A., Jr.; Vreven, T.; Kudin, K. N.; Burant, J. C.; Millam, J. M.; Iyengar, S. S.; Tomasi, J.; Barone, V.; Mennucci, B.; Cossi, M.; Scalmani, G.; Rega, N.; Petersson, G. A.; Nakatsuji, H.; Hada, M.; Ehara, M.; Toyota, K.; Fukuda, R.; Hasegawa, J.; Ishida, M.; Nakajima, T.; Honda, Y.; Kitao, O.; Nakai, H.; Klene, M.; Li, X.; Knox, J. E.; Hratchian, H. P.; Cross, J. B.; Bakken, V.; Adamo, C.; Jaramillo, J.; Gomperts, R.; Stratmann, R. E.; Yazyev, O.; Austin, A. J.; Cammi, R.; Pomelli, C.; Ochterski, J. W.; Ayala, P. Y.; Morokuma, K.; Voth, G. A.; Salvador, P.; Dannenberg, J. J.; Zakrzewski, V. G.; Dapprich, S.; Daniels, A. D.; Strain, M. C.; Farkas, O.; Malick, D. K.; Rabuck, A. D.; Raghavachari, K.; Foresman, J. B.; Ortiz, J. V.; Cui, Q.; Baboul, A. G.; Clifford, S.; Cioslowski, J.; Stefanov, B. B.; Liu, G.; Liashenko, A.; Piskorz, P.; Komaromi, I.; Martin, R. L.; Fox, D. J.; Keith, T.; Al-Laham, M. A.; Peng, C. Y.; Nanayakkara, A.; Challacombe, M.; Gill, P. M. W.; Johnson, B.; Chen, W.; Wong, M. W.; Gonzalez, C.; Pople, J. A. *Gaussian 03*, revision D.01; Gaussian, Inc.: Pittsburgh PA, 2004.

(40) Vest, B.; Varga, Z.; Hargittai, M.; Hermann, A.; Schwerdtfeger, P. *Chem.—Eur. J.* **2008**, *14*, 5130.

Scheme 2. Consecutive Paths for the Formation of Various Metal Chloride Species in RMIm^+Cl^- Ionic Liquids**Table 1.** Gibbs Free Energies at Various Temperatures ($\Delta G_{\text{T}}^\ddagger$, in kJ mol^{-1}) of the Consecutive Formation of Metal (Me is Cr or Cu) Chloride Complexes in MMIm^+Cl^- Model Ionic Liquid (Scheme 2)^a

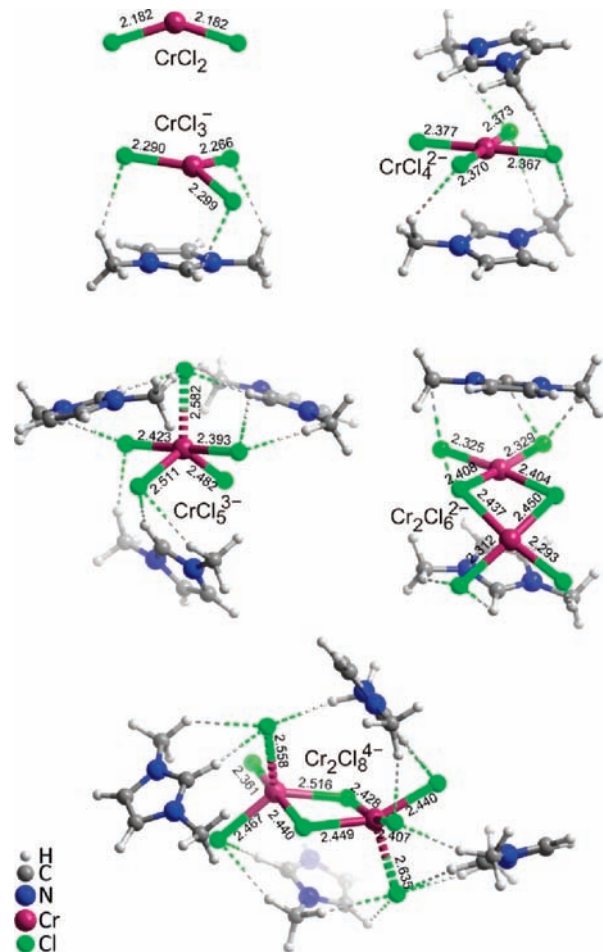
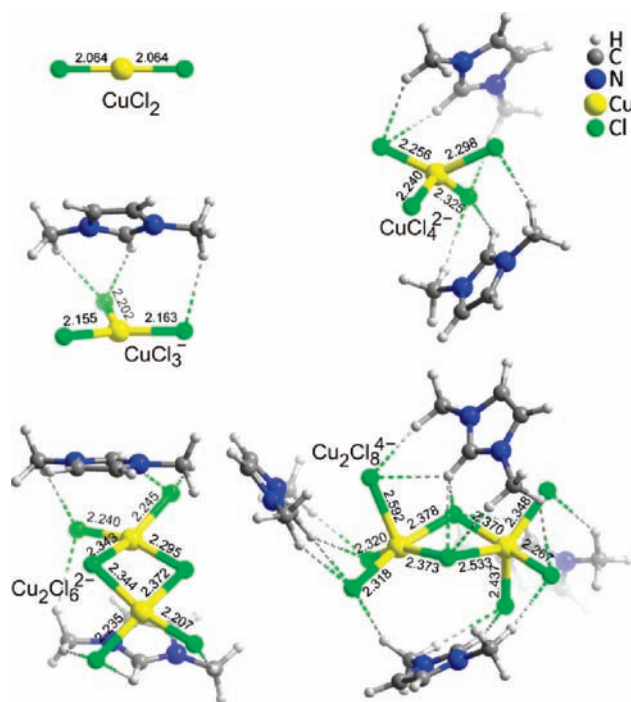
| | $\Delta G_{298\text{K}}^\ddagger$ | $\Delta G_{353\text{K}}^\ddagger$ | $\Delta G_{373\text{K}}^\ddagger$ | $r(\text{Me}-\text{Cl})$ | $r(\text{Me}\cdots\text{Me})$ |
|-------------------------------|-----------------------------------|-----------------------------------|-----------------------------------|--|-------------------------------|
| CrCl_2 | | | | 2.182 | |
| CrCl_3^- | -181 | -130 | -126 | 2.285 | |
| CrCl_4^{2-} | -64 | -90 | -84 | 2.372 (2.386 ^b) | (6.845 ^b) |
| CrCl_5^{3-} | -21 | -2 | 5 | 2.478 | |
| $\text{Cr}_2\text{Cl}_6^{2-}$ | 67 | 51 | 46 | 2.370 | 3.489 |
| $\text{Cr}_2\text{Cl}_8^{4-}$ | 12 | 31 | 38 | 2.470 | 3.643 |
| CuCl_2 | 0 | 0 | 0 | 2.064 | |
| CuCl_3^- | -159 | -153 | -151 | 2.173 | |
| CuCl_4^{2-} | -26 | -8 | -3 | 2.280 (2.286 ^c , 2.280 ^d) | |
| $\text{Cu}_2\text{Cl}_6^{2-}$ | 66 | 51 | 45 | 2.285 | 3.401 |
| $\text{Cu}_2\text{Cl}_8^{4-}$ | 34 | 53 | 60 | 2.394 | 3.547 |

^aThe respective average $\text{Me}-\text{Cl}$ and $\text{Me}\cdots\text{Me}$ distances (r) are given Å. ^bAverage distances computed for the structure directly constructed from the cocrystal. ^cFrom CuCl_5^{3-} model. ^dFrom CuCl_6^{4-} model.

Dutch Belgium Beamline (DUBBLE) of the European Synchrotron Radiation Facility. A Si(111) monochromator was used for these experiments. EXAFS analysis was then performed with EXCURV98⁴¹ on k^3 -weighted unfiltered raw data using the curved wave theory. Phase shifts were derived from ab initio calculations using Hedin-Lundqvist exchange potentials and Von Barth ground states as implemented in EXCURV98. Energy calibrations were carried out with Cr and Cu foils. The amplitude reduction factor S_0^2 associated with central atom shakeup and shake-off effects was set at 0.87 for Cr and 0.8 for Cu. In a typical experiment, 500 mg of EMIm^+Cl^- was mixed with 8 mg metal chloride and 50 mg glucose at 60 °C in a nitrogen-flushed glovebox. Three milliliters of this mixture was transferred into the XAS cell and closed under inert atmosphere. The cells were then transferred to the beamline and EXAFS spectra were recorded of the liquid after heating to 80 °C.

3. Results

3.1. Chloride Complexes. To elucidate the nature and the properties of the stable metal chloride complexes in RMIm^+Cl^- ionic liquid, we performed DFT calculations on the elementary reaction steps representing consecutive addition of model MMIm^+Cl^- ion pairs to MeCl_2 molecule (Me = Cu or Cr) as illustrated in Scheme 2. The possibility of the formation of binuclear metal chloride complexes was also investigated. The relative stabilities of the resulting anionic metal chloride species charge-compensated by sufficient number of MMIm^+ units were correlated with the free energies ($\Delta G_{\text{T}}^\ddagger$, Table 1) of their formation according to Scheme 2. The optimized

**Figure 1.** DFT-optimized structures of chromium chloride complexes in MMIm^+Cl^- model ionic liquid (Cr-Cl distances are in Å).**Figure 2.** DFT-optimized structures of copper chloride complexes in MMIm^+Cl^- model ionic liquid (Cu-Cl distances are in Å).

(41) Binstead, N. *EXCURV98: The Manual*, Daresbury Laboratory: Warrington, UK, 1998.

structures of the corresponding chromium and copper chloride complexes are shown in Figure 1 and 2, respectively.

The initial CrCl_2 monomer has a bent structure (C_{2v} symmetry) with a $\text{Cl}-\text{Cr}-\text{Cl}$ valence angle of 144° and $\text{Cr}-\text{Cl}$ distances of 2.182 Å (Figure 1). This geometry agrees well with the previously reported structure derived from DFT and post-Hartree-Fock calculations.⁴⁰ The computed frequency of the asymmetric stretching vibration (ν_{as}) of CrCl_2 (478 cm^{-1}) is in quantitative agreement with the experimental value (475 cm^{-1}) of gas-phase chromium(II) chloride.⁴²

The interaction of the CrCl_2 with a MMIm^+Cl^- ion pair is strongly favorable ($\Delta G_{373\text{K}}^\circ = -126\text{ kJ mol}^{-1}$) and leads to the formation of a distorted trigonal CrCl_3^- structure. The repulsion between the positively charged Cr center and the charge-compensating MMIm^+ cation induces distortions of the planar trigonal structure, resulting in a substantial deviation of the Cl ligands from the plane of the molecule toward the MMIm^+ moiety. The free energy gain resulting from the addition of another MMIm^+Cl^- and introduction of the fourth Cl^- ligand into the coordination sphere of Cr is approximately 30% lower than the gain upon addition of the first solvent ion pair ($\Delta G_{373\text{K}}^\circ = -84$ and -126 kJ mol^{-1} , respectively). The resulting CrCl_4^{2-} anionic species adopts a square-planar geometry with an average $\text{Cr}-\text{Cl}$ distance of 2.372 Å (Table 1). Further addition of Cl^- anions into the first coordination shell of Cr is temperature dependent. At ambient temperature the formation of a penta-coordinated CrCl_5^{3-} anion is predicted to be thermodynamically favorable, although the free energy gain is rather low (Table 1). However, under typical conditions of sugar conversion ($T > 353\text{K}$),^{9,14} the free energy of the formation of CrCl_5^{3-} species approaches zero and increases further with temperature. This finding suggests that under the experimental conditions such a specific interaction of the CrCl_4^{2-} anion with the ionic liquid is unlikely and is dominated by the nonspecific solvation.

The structure of the CrCl_5^{3-} anionic complex is trigonal bipyramidal, in which the equatorial $\text{Cr}-\text{Cl}$ coordination bonds are somewhat elongated as compared to the axial ones (Figure 1). The substantial deviation (0.1 Å) of the equatorial $\text{Cr}-\text{Cl}$ bond lengths is associated with the inability of the limited number of bulky MMIm^+ cations to form a uniform solvation shell around the anionic Cr complex. This results in an elongation of one of the $\text{Cr}-\text{Cl}$ bonds. Six-coordinated chromium(II) chloride complexes are not formed. Geometry optimization of the initial octahedral CrCl_6^{4-} complex results in the formation of a five-coordinated distorted square-pyramidal chloride complex with a strongly elongated axial $\text{Cr}-\text{Cl}$ coordination. The sixth chloride anion migrates to the second coordination shell.

The rapid decrease of the formation free energies of the CrCl_n complexes with increasing n is associated with the changes in the Lewis acidity of the Cr center. Indeed, whereas the NBO-computed charges on Cl ligands are within the range from -0.45 to -0.6 au for all complexes, the effective charges on the Cr center in CrCl_2 , CrCl_3^- , CrCl_4^{2-} , and CrCl_5^{3-} species are $+0.98$, $+0.40$, $+0.03$,

$+0.01$ au, respectively. This indicates a decreasing Lewis acidity of chromium in line with the substantial elongation of the average $\text{Cr}-\text{Cl}$ distances with increasing coordination number (Table 1).

Similar trends are observed with an increase of the metal-chlorine coordination number in models of copper(II) chloride complexes in the MMIm^+Cl^- ionic liquid. The initial monomeric CuCl_2 is linear ($D_{\infty h}$ symmetry) with $\text{Cu}-\text{Cl}$ distances of 2.064 Å. The optimized geometrical parameters and vibrational frequencies are in line with the previously reported experimental⁴³ and high-level ab initio theoretical studies.⁴⁴ The calculated free energy of solvation of CuCl_2 with a single MMIm^+Cl^- ion pair is on average higher by 20 kJ mol^{-1} than the corresponding values in the Cr case. The geometries of three-coordinated complexes are similar for both metals. The coordination properties and the relative stability of the four-coordinated CuCl_4^{2-} species are very different from that of the CrCl_4^{2-} one. CuCl_4^{2-} forms a perturbed tetrahedral complex with valence $\text{Cl}-\text{Cu}-\text{Cl}$ angles equal to 133 and 103° . Attempts to extend the coordination sphere of Cu^{II} by introducing further MMIm^+Cl^- ion pairs were not successful. Geometry optimizations of the pyramidal and bipyramidal CuCl_5^{3-} and the octahedral CuCl_6^{4-} anions charge-compensated by an appropriate number of MMIm^+ cations result in the isolated perturbed tetrahedral CuCl_4^{2-} complexes with MMIm^+ and excessive Cl^- species located in the second coordination sphere of Cu. These theoretical findings are in agreement with the structural properties of Cu^{2+} species in a $\text{CuCl}_4^{2-}(\text{BMIm}^+)_2$ crystal.²⁷ The geometrical parameters of the copper tetrachloride core in all these structures are very similar (Table 1). Average optimized $\text{Cu}-\text{Cl}$ distances are 2.28 Å. NBO charges of $+0.79$, $+0.68$, and $+0.53$ were computed for Cu centers in CuCl_2 , CuCl_3^- , and CuCl_4^{2-} , respectively.

Besides the coordination to additional MMIm^+Cl^- solvent ion pairs, the mononuclear metal chloride complexes can in principle interact with each other resulting in binuclear complexes. Two reaction paths to their formation were considered, starting from the most stable MeCl_4^{2-} species (Scheme 2). The first path involves the substitution of two Cl^- ligands with another MeCl_4^{2-} species resulting in the formation of $\text{Cr}_2\text{Cl}_6^{2-}$ and $\text{Cu}_2\text{Cl}_6^{2-}$ cores (Figures 1 and 2) with two bridging Cl anions. Both metal centers in these complexes remain four-coordinated by chlorine ligands. This geometry closely resembles that of the optimized mononuclear species. The most notable change upon the formation of binuclear complexes is the elongation of the $\text{Me}-\text{Cl}$ bonds with the bridging ligands. This is because of the decreased basicity of the Cl^- anions interacting with two cationic centers. In support of this are the computed NBO charges on the respective bridging anions, which become more positively charged by 0.20 and 0.14 au (respectively, for $\text{Cr}_2\text{Cl}_6^{2-}$ and $\text{Cu}_2\text{Cl}_6^{2-}$ species) as compared to the terminal Cl.

The second dimerization path involves the expansion of the coordination shell of the MeCl_4^{2-} species upon the

(43) Lorenz, M.; Caspary, N.; Foeller, W.; Agreiter, J.; Smith, A. M.; Bondybey, V. E. *Mol. Phys.* **1997**, *91*, 483.

(44) Zou, W.; Boggs, J. E. *J. Chem. Phys.* **2009**, *130*, 154313, and references therein.

(42) Kovba, V. M. *Zh. Neorg. Khim.* **1983**, *28*, 2689.

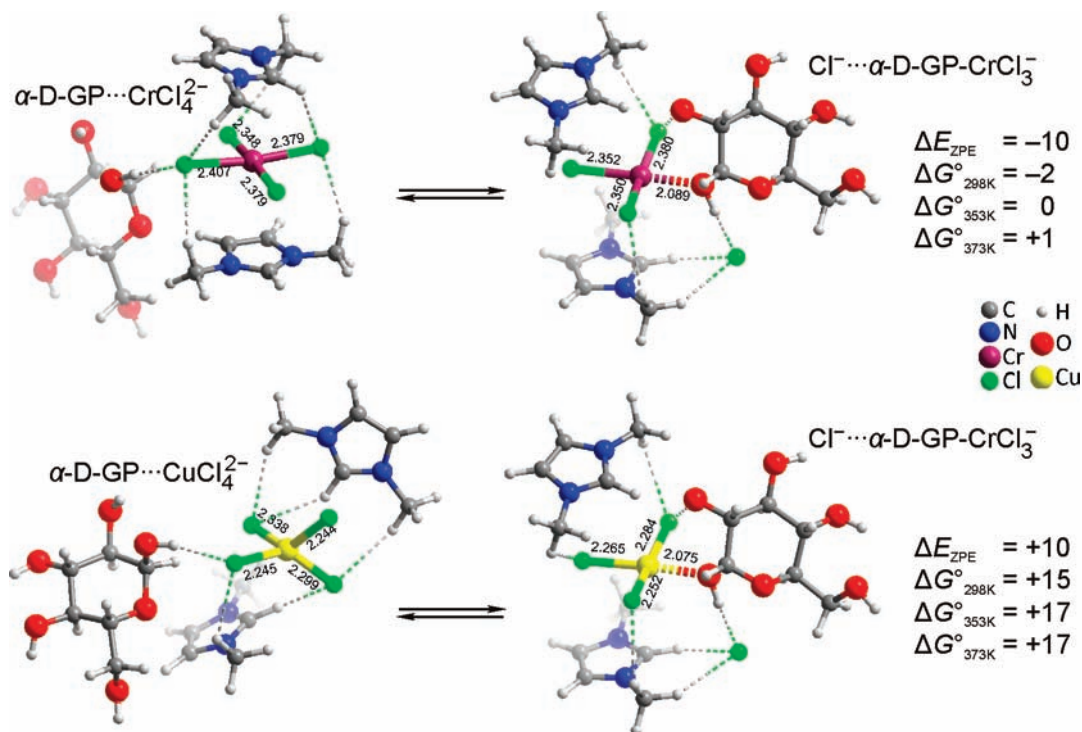


Figure 3. Optimized structures of hydrogen bonded (left) and directly coordinated (right) glucose to Cr^{II} and Cu^{II} chlorides in MMImCl model ionic liquid. ZPE-corrected energies and free energies at different temperatures computed for the respective interconversions are given in kJ mol^{-1} .

interaction of two mononuclear complexes. This leads to the formation of five-coordinated metal centers interconnected via two Cl^- bridges. Although monomeric copper chlorides with five Cl^- ligands in the first coordination sphere of copper were not identified, the formation of five-coordinated metal centers in a binuclear complex is in principle possible. Both trigonal bipyramidal and square pyramidal geometries of metal centers are realized in each of the complexes ($\text{Cr}_2\text{Cl}_8^{4-}$ and $\text{Cu}_2\text{Cl}_8^{4-}$, respectively Figure 1 and 2). Nevertheless, the average metal–chloride bond distances and coordination numbers in binuclear complexes are close to those found for their mononuclear counterparts (Table 1).

Although these binuclear structures represent stable species, the calculated ΔG° values indicate that the dimerization is strongly unfavorable (Table 1). Note that in this case, the initial models for the respective binuclear complexes were constructed in such a way that all $\text{Me}-\text{Cl}$ bonds with either bridging or terminal ligands were equal to the bond lengths in the respective monomeric MeCl_2 molecules. An alternative approach¹⁴ is to construct a model for the binuclear chromium(II) chloride complex based on the experimental X-ray diffraction data of a cocrystal of EMIm^+Cl^- and CrCl_2 .³⁴ In this case geometry optimization resulted in a structure containing two distant square-planar CrCl_4^{2-} moieties ($r(\text{Cr}\cdots\text{Cr}) = 6.845 \text{ \AA}$).¹⁴ The geometrical parameters of each of the species formed are very close to those computed for the isolated CrCl_4^{2-} complex (Table 1).

3.2. Glucose Coordination. To analyze the possibility of coordination of glucose to chloride complexes of Cu^{2+} and Cr^{2+} in RMIm^+Cl^- , the energetics of the introduction of α -D-glucopyranose (α -D-GP) into the first coordination sphere of the metal center was investigated. To minimize potential computational errors, such as basis set

superposition error and nonuniform charge-compensation within the finite size molecular models, we considered the equilibrium between two isomeric structures representing the “coordinated” and “noncoordinated” situations. α -D-GP either forms a hydrogen bond with the metal chloride complex or substitutes one of the Cl^- ligands. A single coordination mode of glucose, namely that to O1 hydroxyl group (Scheme 1), was considered in this case. Such coordination is a precursor for the selective transformations of glucose.¹⁴ The energetics for the interconversion between the coordinated and noncoordinated states of α -D-GP with Cu^{2+} and Cr^{2+} chloride complexes and the respective optimized structures are summarized in Figure 3.

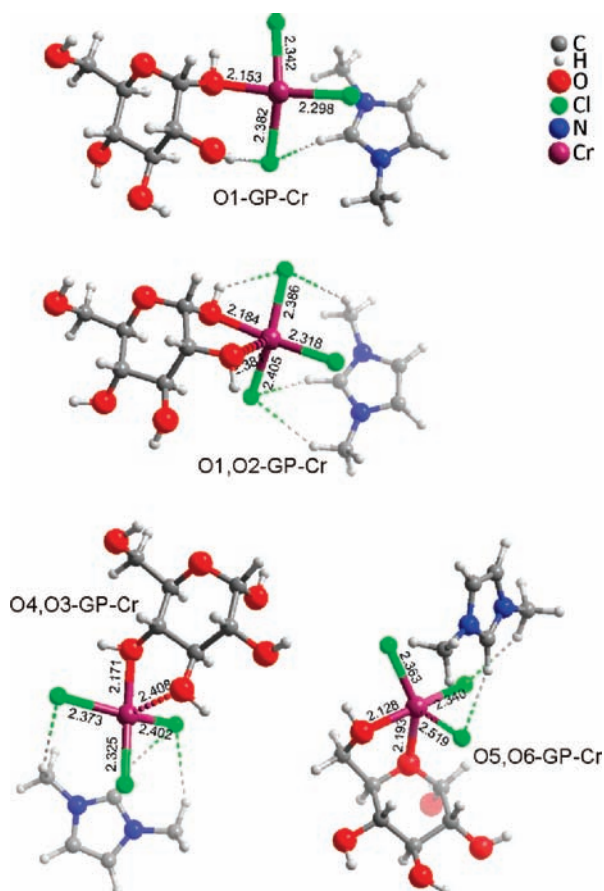
Note that the initial models for the noncoordinated and coordinated states of glucose complexes were similar for both metals considered here. For the hydrogen-bonded models (noncoordinated state), the geometry optimization leads to distinct coordination environments established around Cr^{2+} and Cu^{2+} centers closely resembling those discussed above for the isolated chlorides. When glucose is introduced into the first coordination sphere of the metal, the resulting geometries become similar for both metals (Figure 3). The three remaining Cl^- ligands and the O1H moiety of the carbohydrate form a perturbed square planar complex. The degree of structural perturbations in the copper complex is larger than in the chromium one. Whereas the angles formed by the opposing ligands in α -D-GP $\cdots\text{CrCl}_3^-$ are close to 180° , the corresponding $\text{O}-\text{Cu}-\text{Cl}$ and $\text{Cl}-\text{Cu}-\text{Cl}$ angles in α -D-GP $\cdots\text{CuCl}_3^-$ structure are below 170° .

A distinct difference between bivalent chromium and copper in the ability to coordinate the carbohydrate is apparent from the computed energetics for the interconversion of the noncoordinated and coordinated glucose

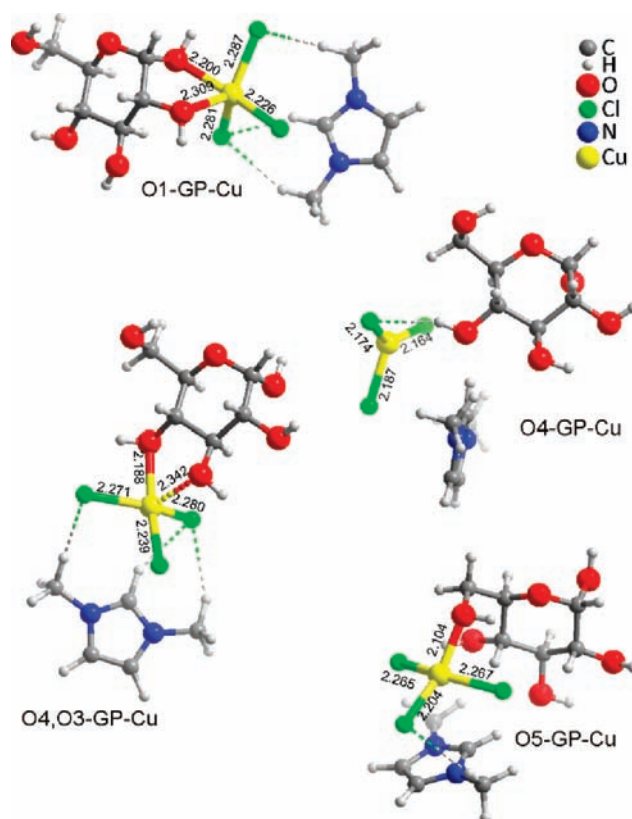
Table 2. Relative Stabilities (ΔE_{ZPE} , $\Delta G_{353\text{K}}^{\circ}$ in kJ mol^{-1}) and Average Metal–Chlorine and Metal–Oxygen Distances (all in Å) for Different Coordination Modes of α -D-Glucopyranose with MeCl_3^- (Me = Cr or Cu)

| coordination mode | chromium(II) | | | | copper(II) | | | |
|-----------------------------------|-------------------------|----------------------------------|--------------------------------|--------------------------|-------------------------|----------------------------------|--------------------------------|--------------------------|
| | ΔE_{ZPE} | $\Delta G_{353\text{K}}^{\circ}$ | $r(\text{Cr}\cdots\text{O})^a$ | $r(\text{Cr}-\text{Cl})$ | ΔE_{ZPE} | $\Delta G_{353\text{K}}^{\circ}$ | $r(\text{Cu}\cdots\text{O})^a$ | $r(\text{Cu}-\text{Cl})$ |
| O1 | 9 | 9 | 2.153 | 2.341 | | | | |
| O1,O2 | 0 | 0 | 2.184 (2.381) | 2.370 | 0 | 0 | 2.200, (2.309) | 2.264 |
| O2,O1 | 10 | 9 | 2.168 (2.369) | 2.362 | 10 | 8 | 2.173 (2.331) | 2.263 |
| O2,O3 | 12 | 12 | 2.171 (2.410) | 2.366 | | | | |
| O3 | | | | | 9 | 5 | 2.075 | 2.245 |
| O3,O4 | 15 | 15 | 2.133 (2.605) | 2.363 | | | | |
| O4,O3 (enzyme-like) ¹⁶ | 16 | 14 | 2.171 (2.408) | 2.367 | 17 | 10 | 2.188 (2.342) | 2.263 |
| O4 | 31 | 25 | 2.128 | 2.338 | 16 | 5 | 2.175 | 2.175 |
| O5 | -13 | 7 | 2.128 | 2.342 | -14 | -2 | 2.104 | 2.245 |
| O5,O6 | -2 | 1 | 2.128 (2.193) | 2.366 | 0 | 14 | 2.124 (2.347) | 2.276 |

^a Bond length of the secondary coordination is given in parentheses.

**Figure 4.** Selected coordination modes of α -D-glucopyranose to CrCl_3^- species charge-compensated by a single MIm^+ cation.

complexes (Figure 3). The reaction is exothermic by 10 kJ mol^{-1} for Cr^{II} . The calculated ΔG values (Figure 3) indicate that there is an equilibrium between the isolated CrCl_4^{2-} and $\alpha\text{-D-GP}\cdots\text{CrCl}_3^-$ complexes in the ionic liquid medium. In contrast, the coordination of glucose to Cu^{2+} is unfavorable. Therefore, the unexpected planar Cu coordination in $\alpha\text{-D-GP}\cdots\text{CuCl}_3^-$ can be explained by the combination of two factors, namely, the ease of the removal of the fourth chlorine ligand from the coordination sphere of copper and the weakness of the interaction of the Cu^{II} center with the hydroxyl group of glucose. This is also evident from the comparison of the strengths of donor–acceptor electron interactions derived from the

**Figure 5.** Selected coordination modes of α -D-glucopyranose to CuCl_3^- species charge-compensated by a single MIm^+ cation.

NBO analysis. The total energy of all interactions between the metal chloride and the carbohydrate in the case of copper complexes is approximately two times lower than that estimated for the chromium complex. The rather short $\text{Cu}\cdots\text{O}$ contact in $\alpha\text{-D-GP}\cdots\text{CuCl}_3^-$ is because of the formation of a hydrogen bonding network involving the hydroxyl groups of the carbohydrate, charge-compensating MIm^+ cations and the Cl^- ligands (Figure 3).

We further analyzed the potential influence of the coordination to different hydroxyl groups of the sugar molecule by considering various coordination modes using a simplified model consisting of $\alpha\text{-D-GP}$, a MeCl_3^- anion, and a single MIm^+ cation to ensure charge neutrality. The relative stabilities and the selected structural parameters are summarized in Table 2 and selected optimized structures are shown in Figures 4 and 5.

The DFT-computed free energy differences between various coordination modes of glucose are within ~ 15 kJ mol $^{-1}$ for both metals. The only exception is the coordination of glucose at its O4 position to CrCl $_3^-$. This structure is less stable by 25 kJ mol $^{-1}$ compared to the most favorable O1,O2 mode. Taking into account the general accuracy of DFT⁴⁵ of approximately 10 kJ mol $^{-1}$ and the limited number of explicitly included solvent pair considered in this analysis, these differences are minor and probably not significant. This is further supported by the finding that minor perturbations of the initial model may cause deviations in the free energies in the order of 10 kJ mol $^{-1}$. As an example, two possible configurations (O1-GP and O1,O2-GP) of the glucose complex with CrCl $_3^-$ with the primary O1 coordination are shown in Figure 4. The main difference between these structures is the presence of an additional Cr \cdots O2 contact in the latter structure. The formation of this contact upon the geometry optimization is controlled by the conformation of the O2H group in the initial model. A comparison of the optimized structures for various complexation modes of glucose to Cu and Cr chlorides suggests that for both metals very similar coordination environments are formed. Most of the structures obtained show either distorted square planar or square pyramidal configuration (Figures 4 and 5). The latter usually originates from a four-coordinated complex by formation of a secondary coordination interaction between the metal center and a neighboring OH group of the carbohydrate. No apparent correlation between the number of metal–carbohydrate interactions, geometrical properties and the relative stabilities of the complexes is found (Table 2).

The coordination of a metal species to the O1 site of glucose is usually considered to be essential for its chemocatalytic activation in ionic liquids.^{9–14} In biocatalytic systems another coordination mode, namely O4,O3 is usually considered. No preference for the latter follows from the computational results. Moreover, whereas the binding modes involving the O1–Me coordination are among the most stable ones, the O4,O3-binding destabilizes the complexes.

The computational analysis of possible coordination modes of glucose with Cu provided further support for the above proposition of weak interaction between the neutral α -D-GP and Cu $^{2+}$ cations. Upon the geometry optimization of one of the structures, namely O4-GP-Cu (Figure 5), the Cu \cdots O interaction disappears and a trigonal CuCl $_3$ species hydrogen-bonded to the carbohydrate is formed. The formation free energy of the resulting structure is only 5 kJ mol $^{-1}$ higher compared to that of the most stable complex (Table 2).

3.3. XAS Study of Cu II and Cr II Complexes in EMIm $^+$ Cl $^-$ Ionic Liquid. To support and validate the computational results presented above, structural information about the Cr and Cu coordination complexes formed in the ionic liquid medium was obtained from extended X-ray absorption fine structure (EXAFS) spectra at the Cr and Cu K-edge, respectively (Figure 6). Table 3 lists the EXAFS fit parameters for CrCl $_2$ and CuCl $_2$ dissolved in EMIm $^+$ Cl $^-$ ionic liquid at 80 °C prior and after the addition of glucose.

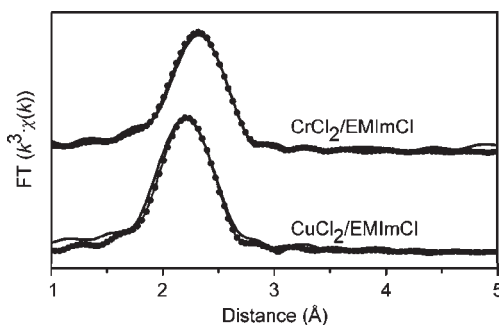


Figure 6. Fourier transforms of EXAFS spectra and their simulations for CrCl $_2$ and CuCl $_2$ in EMIm $^+$ Cl $^-$ ionic liquid at 80 °C.

Table 3. EXAFS Fit Parameters^a of the MeCl $_2$ /EMIm $^+$ Cl $^-$ Systems

| backscatterer | edge, eV | <i>N</i> | <i>r</i> , Å | $\Delta\sigma^2$, Å 2 | ΔE^0 , eV |
|--------------------------------------|---------------|-------------------------------------|--------------|---------------------------|-------------------|
| CrCl $_2$ /EMIm $^+$ Cl $^-$ | | | | | |
| Cr–Cl | 5993.1 | 3.9 | 2.39 | 0.008 | –8.4 |
| CuCl $_2$ /EMIm $^+$ Cl $^-$ | | | | | |
| Cu–Cl | 8984.8 | 4.1 | 2.28 | 0.016 | 0.0 |
| glucose/CrCl $_2$ /EMIm $^+$ Cl $^-$ | | | | | |
| Cr–Cl | 5993.1 | 2.9 | 2.38 | 0.007 | –3.4 |
| Cr–O | | 1.0 | 2.13 | 0.015 | |
| glucose/CuCl $_2$ /EMIm $^+$ Cl $^-$ | | | | | |
| Cu–Cl | ~ 8984.6 | 2.0 ^b , 4.0 ^c | 2.23 | 0.011 | –5.5 |
| Cu–O | | | | | |

^a Coordination number (*N*) \pm 20%; coordination distance (*R*) \pm 0.02 Å, Debye–Waller factor ($\Delta\sigma^2$) \pm 10%; inner potential (ΔE^0). ^b Assuming Cu $^{2+}$. ^c Assuming Cu $^+$.

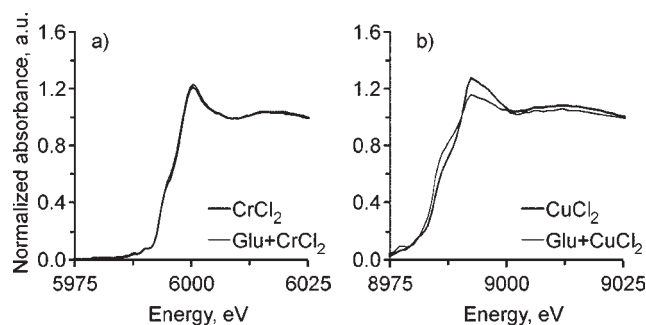


Figure 7. XANES spectra for (a) CrCl $_2$ and (b) CuCl $_2$ in EMIm $^+$ Cl $^-$ ionic liquid in the presence and in the absence of glucose (measurements at 80 °C).

The corresponding XAS spectra are shown in Figure 7. For both metals, before the sugar was introduced to the solution, four Cl ligands were detected at a distance of 2.39 and 2.28 Å, respectively for Cr II and Cu II species.

EXAFS measurements in the presence of glucose evidence for coordination of chromium to the carbohydrate via one of its hydroxyl groups (Table 3). One of the chlorine ligands in the coordination sphere of Cr is substituted by an O-containing ligand. The resulting Cr–O and Cr–Cl distances are, respectively, 2.13 and 2.38 Å, in agreement with the results of DFT calculations (Table 2). The edge position in the Cr K-edge XANES spectra both in the presence and in the absence of sugar

(45) Olsen, R. A.; Philipsen, P. H. T.; Baerends, E. J. *J. Chem. Phys.* **2003**, *119*, 4522.

was 5993.1 eV. The respective value for the reference pure CrCl_2 is 5994.9 eV. This implies that Cr ions remain in the +2 oxidation state.

A different coordination behavior of copper is observed in a similar experiment. The introduction of glucose does not result in its coordination with Cu. Assuming that all copper ions in the solution remain in the +2 formal oxidation state, an unrealistically low Cu–Cl (for Cu^{II} compounds) coordination number of 2 is obtained from the EXAFS fit. However, if we assume that all Cu ions are in the +1 state, the Cu–Cl coordination number will be four because of the difference in the amplitude reduction factor between CuCl and CuCl_2 . This suggests that upon the glucose addition bivalent copper (partially) reduces to Cu^{I} . Indeed, the analysis of the near-edge structure of the XAS spectra reveals substantial changes upon the addition of sugar. Whereas a distinct edge position at 8984.8 eV is observed for $\text{CuCl}_2/\text{EMIm}^+\text{Cl}^-$ (the reference value for pure CuCl_2 is 8985.5 eV), the addition of sugar to the solution results in the formation of features in the XAS spectra at lower energies that indicate (partial) reduction of Cu^{2+} to Cu^+ (Figure 7b). This is in line with the results of the coloration experiments (see Supporting Information), in which a notable decrease of the color intensity of the copper-containing solution was observed after the addition of glucose.

Summarizing, the XAS results clearly indicate that the isolated MeCl_4^{2-} (Me = Cr or Cu) anions are the dominant metal-containing complexes in the EMIm^+Cl^- ionic liquid solutions in the absence of glucose. This coheres very well with the predictions of DFT calculations (see section 3.1). The interatomic distances derived from the EXAFS measurements (Table 3) are in a very good agreement with the optimized structural parameters of the most stable CrCl_4^{2-} and CuCl_4^{2-} species (Table 1). The spectroscopic changes observed upon the introduction of the sugar substrate to the metal chloride/ionic liquid systems are also in line with the theoretical results. Indeed, the formation of a metal chloride–carbohydrate coordination complex is evident only in the case of CrCl_2 , whereas no qualitative changes in the coordination environment of copper are observed (Table 3). Interestingly, despite the absence of a direct interaction between the copper centers and the sugar from XAS and DFT, the sugar is apparently able to induce a fast reduction of Cu^{2+} cations.

4. Discussion

Rational design of novel and improved catalytic systems for chemical transformations of lignocellulosic biomass requires insight into the structural and coordination properties of the catalytically relevant species, as well as molecular level understanding of their complexation with carbohydrates. Some studies^{9–13} on the ionic liquid-mediated glucose dehydration by metal chlorides have presented tentative schemes for the reaction mechanism. Several mechanisms suggest the direct involvement of the cationic (RMIm^+) organic moieties of the ionic liquid in the reactive metal-containing complexes.^{9,13} Such a picture suggests that chemical and catalytic properties of metal centers can directly be affected by manipulating the size and structure of the RMIm^+ part of the solvent.

The results presented in this study contradict this supposition. No coordination of the organic part of the ionic liquid has been found in complexes with Cu^{2+} or Cr^{2+} (Figure 1 and 2). These computational results are confirmed by the absence of metal···carbon coordination in the EXAFS spectra. The spontaneous formation of metal-carbene complexes in RMIm^+Cl^- ionic liquids is rather unrealistic because of the much higher acidity of the resulting HCl molecules as compared to that of the dialkylimidazolium cation.

The DFT-computed relative stabilities of mononuclear chromium(II) and copper(II) chloride complexes in a model MMIm^+Cl^- ionic liquid (Table 1) indicate that the four-coordinated MeCl_4^{2-} anions charge-compensated by two RMIm^+ cations are the dominant species in solution. The structural properties of such complexes are in a perfect agreement with the EXAFS fit results (Figure 6, Table 3). This result is also in line with a previous electrochemical study on the behavior of chromium chlorides in basic aluminum-containing EMIm^+Cl^- molten salts,⁴⁶ where it has been found that two EMIm^+Cl^- molecules per Cr^{2+} are required to completely dissolve CrCl_2 . Thus, the resulting chromium chloride complexes must have a Cr to Cl ratio of 4. No conclusion on the nuclearity of the thus formed complexes can be deduced from these data. It should be noted that mononuclear Cr species are commonly assumed as being relevant for catalytic transformations of sugars.^{9–11} It is known that other metal ions, such as aluminum,⁴⁷ hafnium, and zirconium,³³ may form binuclear chloride complexes in dialkylimidazolium-based ionic liquids. The results presented above rule out such a possibility for the cases of dilute solutions of CuCl_2 and CrCl_2 . In both cases the self-organization of stable mononuclear chloride complexes into binuclear structures is thermodynamically unfavorable (Table 1) and has not been observed by EXAFS spectroscopy. This implies that the formation of binuclear chromium(II) complexes necessary for the selective glucose dehydration¹⁴ is indeed transient in nature and can only occur in the presence of very specific activated sugar intermediates in solution.

Selective catalytic transformation of sugars requires specific coordination of the reactant to a metal complex. The mechanism for glucose dehydration to HMF involves fructose formation as a crucial reaction intermediate that proceeds via the open form of the sugar, in which an H-shift between C2 and C1 atoms takes place to yield fructose.¹⁴ Opening of the glucopyranose ring is initiated by the deprotonation of O1H moiety followed by a proton transfer to the O6 position of glucose. This step is promoted by the coordination of a Lewis acidic metal center to the O1 site of the sugar. The bidentate O1,O2 coordination mode is necessary for catalyzing the rate-limiting H-shift step in glucose isomerization.¹⁴ Most of the proposed mechanistic schemes assume such a coordination mode of glucose to be specific for the successful dehydration catalyst.^{9,11,13}

On the other hand, there is no apparent reason to consider the coordination properties and intrinsic reactivity of O1H and O2H to be drastically different from other hydroxyl groups of glucose. According to our model DFT calculations coordination modes involving less sterically hindered OH sites can show comparable stability to the O1,O2 binding

(46) Liu, J. S.-Y.; Chen, P.-Y.; Sun, I.-W. *J. Electrochem. Soc.* **1997**, *144*, 2388.

(47) Zhang, Z. C. *Adv. Catal.* **2006**, *49*, 153.

mode for both Cr^{2+} and Cu^{2+} . It is interesting to note some preference of copper ions to form monodentate complexes with glucose resulting in a substantially larger number of potential coordination modes with similar stability. In the case of chromium(II) chloride bidentate complexes are generally preferred. This leads to a substantial effect of the relative orientation of OH groups of glucose on the stability of the respective coordination complex with Cr^{2+} . Nevertheless, the energy differences between most of different glucose complexes with either copper or chromium do not exceed 10–15 kJ/mol. These are too low to convincingly conclude on the exclusive formation of a particular coordination mode.

Despite the very similar picture of geometrical properties and relative stabilities of the sugar complexes for Cu^{2+} and Cr^{2+} , the thermodynamics of their formation from the respective MeCl_4^{2-} species differs substantially. The exchange of Cl^- ligand by glucose in the coordination sphere of CuCl_4^{2-} is endothermic and characterized by unfavorable values of Gibbs free energy. In contrast, such a process in the case of chromium(II) chloride complexes is thermodynamically favored (Figure 3). These computational predictions are in line with the results of XAS experiments. Indeed, only in the case of $\text{CrCl}_2/\text{EMIm}^+\text{Cl}^-$ system, oxygen neighbors were detected in the coordination sphere of the metal center upon the introduction of glucose.

Such a different coordination behavior of Cu^{2+} and Cr^{2+} can be indirectly deduced from previously reported data. Zhang et al. reported ^1H NMR spectra of glucose in EMIm^+Cl^- in the presence of CrCl_2 and CuCl_2 .⁹ Note that both metal ions are paramagnetic and their direct binding to the sugar would strongly influence the NMR results. Indeed, in the presence of Cr^{2+} cations no useful information could be obtained from NMR, because of severe line broadening. This observation is consistent with the predicted ability of Cr^{2+} to form stable coordination complexes with the sugar molecules. Furthermore, the fast ligand exchange in the resulting complexes and nonspecificity of the coordination with respect to the hydroxyl groups of glucose will have a great impact on all of the protons in the ^1H NMR spectrum. The spectra of the Glucose/ $\text{CuCl}_2/\text{EMIm}^+\text{Cl}^-$ system were affected to a much lesser extent.⁹ The presence of Cu^{2+} resulted in the broadening and upfield shift of $-\text{OH}$ resonances only. These observations can be explained by the preference of paramagnetic CuCl_4^{2-} species to form hydrogen bonded complexes with the sugar substrate. As a result the effect of such interactions on the C–H resonances is expected to be minor, if any, in agreement with the ^1H NMR observations.⁹

These molecular-level insights into the coordination behavior of copper(II) and chromium(II) chlorides in EMIm^+Cl^- ionic liquids allow rationalization of their catalytic reactivity toward glucose activation. It has previously been reported that both metal chlorides are able to promote mutarotation of glucose that involves the glucopyranose ring-opening.^{9,14} However, only Cr^{2+} can catalyze further isomerization to fructose that is required for the selective HMF production. It appears that such a unique catalytic behavior of CrCl_2 is directly related to its ability to coordinate the sugar substrate providing thus the necessary stabilizing environment that facilitates the isomerization reaction. The finding that the free energy of the sugar to Cl^- ligand exchange process is close to zero in the case of Cr^{2+} is also important.

One expects that, if glucose binding to a Lewis acidic site was irreversible, the activation of the sugar substrate would occur at various OH sites, resulting in nonselective conversion. On the other hand, the coordination of the sugar to the metal chloride is a prerequisite to its activation. This does not appear to be the case for copper(II) chloride. Although in this case no $\text{Cu}\cdots\text{OH}$ coordination bonds are formed, $\text{Cu}^{\text{II}}\text{Cl}_2$ is active in activation of glucose, resulting in mutarotation and ultimately in almost complete glucose conversion to other products than the desirable HMF one.⁹ The latter is probably due to the oxidation of glucose by Cu^{2+} . The reduction of Cu^{2+} to Cu^+ requires the presence of the open form of the sugar in the reaction medium. The open form of glucose is an aldehyde, which can be oxidized in the presence of water to a carboxylic acid. This ultimately leads to catalyst deactivation, as Cu^+ is inactive in glucose conversion.⁹ The acid produced upon this side-reaction will catalyze nonselective formation of humins and other undesired products. This implies that prior to the catalyst reduction to Cu^+ and glucose oxidation, both the glucopyranose ring-opening and partial dehydration of the sugar must take place. The exact molecular mechanism of the initial glucose activation by CuCl_4^{2-} is not clear. Nevertheless, we can speculate that the glucopyranose ring-opening in this case proceeds via an attack of CuCl_4^{2-} species by O1H site of glucose, resulting in the formation of tricoordinate CuCl_3^- anion and HCl. In line with this supposition, DFT calculations predict a high mobility of the fourth chlorine ligand in CuCl_4^{2-} (Table 1). The formation of stable CuCl_3^- species (O4-GP-Cu, Figure 5) has also been found when different coordination modes of Cu were considered. The product HCl reprotonates the sugar intermediate at the O6 site, resulting in the formation of the open form of glucose and the regeneration of CuCl_4^{2-} . In principle, a similar mechanism can be proposed for the initial dehydration reactions. In this case the selective attack by O1H site is probably not necessary.

5. Conclusion

Model DFT calculations indicate that four-coordinated MeCl_4^{2-} complexes are the dominant species formed by the interaction of copper(II) and chromium(II) chlorides with dialkylimidazolium chloride ionic liquid. The structural properties of these species depend strongly on the nature of the metal center. Whereas perturbed tetrahedral complex is formed in the case of Cu^{2+} , a square-planar structure is preferred for Cr^{2+} . For both metal ions, the formation of binuclear chloride complexes is thermodynamically unfavorable in dilute solutions. No chemical bonding between the metal centers and cationic RMIm^+ part of the ionic liquid solvent was detected in all of the species considered. The theoretical results are in a perfect agreement with the experimental XAS data.

The substitution of a Cl^- ligand by glucose molecule in a stable MeCl_4^{2-} complex is feasible only in the case of bivalent chromium. The predicted free energy change for this reaction is close to 0 at the reaction conditions. The resulting fast ligand exchange is crucial for the high selectivity of glucose activation by $\text{CrCl}_2/\text{EMIm}^+\text{Cl}^-$ because of the low specificity of chromium chloride complex toward coordination to different hydroxyl groups of the substrate. The formation of glucose–chromium(II) chloride coordination complexes is evidenced from EXAFS experiments.

In the case of copper(II), the introduction of glucose into the coordination sphere of Cu^{2+} centers is thermodynamically unfavorable. The promotion effect of CuCl_2 on the glucopyranose ring-opening, mutarotation and potential low-selective dehydration paths are explained by the high mobility of basic Cl^- ligands in the dominant CuCl_4^{2-} species and substantial predicted stability of under-coordinated CuCl_3^- species. XAS measurements indicate reduction of bivalent copper species in the presence of glucose already at 80 °C. High glucose conversion by CuCl_2 is most likely associated with the oxidation of the sugar substrate and reduction of the active species to Cu^+ .

Acknowledgment. This research has been performed within the framework of the CatchBio program. The authors gratefully acknowledge the support of the Smart Mix Program of The Netherlands Ministry of Economic Affairs and The Netherlands Ministry of Education, Culture and Science. NCF is acknowledged for providing computational resources with financial support from NWO.

Supporting Information Available: Supplementary experimental details. This material is available free of charge via the Internet at <http://pubs.acs.org>.